Research Repository UCD

Title	Non-destructive determination of collagen fibril width in extruded collagen fibres by piezoresponse force microscopy
Authors(s)	Bazaid, Arwa, Neumayer, Sabine M., Sorushanova, Anna, Guyonnet, Jill, Zeugolis, Dimitrios I., Rodriguez, Brian J.
Publication date	2017-09-13
Publication information	Bazaid, Arwa, Sabine M. Neumayer, Anna Sorushanova, Jill Guyonnet, Dimitrios I. Zeugolis, and Brian J. Rodriguez. "Non-Destructive Determination of Collagen Fibril Width in Extruded Collagen Fibres by Piezoresponse Force Microscopy." IOP Publishing, September 13, 2017. https://doi.org/10.1088/2057-1976/aa85ec.
Publisher	IOP Publishing
Item record/more information	http://hdl.handle.net/10197/11195
Publisher's version (DOI)	10.1088/2057-1976/aa85ec

Downloaded 2026-05-01 23:42:07

The UCD community has made this article openly available. Please share how this access benefits you. Your story matters! (@ucd_oa)

© Some rights reserved. For more information

Non-destructive determination of collagen fibril width in extruded collagen fibres by piezoresponse force microscopy

Arwa Bazaid[1], Sabine M. Neumayer[1], Anna Sorushanova[2], Jill Guyonnet[1], Dimitrios Zeugolis[2] and Brian J. Rodriguez[1]

[1]School of Physics & Conway Institute of Biomolecular and Biomedical Research, University College Dublin, Belfield, Dublin 4, Ireland

[2]Regenerative, Modular & Developmental Engineering Laboratory (REMODEL) & Science Foundation Ireland (SFI) Centre for Research in Medical Devices (CÚRAM), National University of Ireland Galway (NUI Galway), Galway, Ireland

E-mail: brian.rodriguez@ucd.ie

Keywords: collagen, biomaterials, extrusion, AFM, piezoelectricity, PFM, electromechanical coupling

Abstract

Extruded collagen fibres are a promising platform for tissue engineering applications. Ensuring that the functional properties of the engineered tissues possess similar structural properties as native tissues is important for biomedical applications. Advanced imaging tools including scanning electron microscopy (SEM) and atomic force microscopy (AFM) have revealed the structural features of collagen fibrils within such fibres; however, these techniques often require modification steps that can alter the sample in the process. Here, lateral piezoresponse force microscopy (LPFM), which

is sensitive to the polar orientation of piezoelectric collagen fibrils, is demonstrated as a promising tool to assess the width of individual fibrils and moreover map their organisation and polar orientation without altering the sample. Within the fibres studied, the collagen fibrils showed a highly anisotropic arrangement with preferred alignment along the length of the fibre. Fibril widths of 74 ± 18 nm and 73 ± 19 nm in untreated and bleached fibres, respectively, were measured from LPFM amplitude images. These values agreed with values from SEM (70 ± 10 nm) and AFM (71 ± 19 nm) measurements that could only be obtained from bleached fibres.

1. Introduction

Collagen-based scaffolds that possess similar functional properties to native tissues provide a promising template for tissue engineering applications such as nerve repair, wound healing, and vascular grafts [1–5]. Fibril size and organisation significantly affect the properties of such scaffolds and recent efforts to optimise the structural properties of extruded collagen fibres have been made [6–11]. Scanning electron microscopy (SEM), transmission electron microscopy (TEM), X-ray diffraction (XRD), and atomic force microscopy (AFM) have all been used successfully to measure structural properties of collagen, revealing such properties as D periodicity and fibril size and alignment. Depending on the sample and information desired, destructive sample preparation may be required. For instance, SEM is typically operated in vacuum, requires surface coating, and collagen samples are sometimes subjected to chemical treatments including bleaching, which may alter the structure [12, 13]. TEM is operated in vacuum, samples must be transparent to electrons, and staining is required to determine fibril polarity, as defined by the amino- (N) and carboxylic (C) termini of the constituent collagen molecules [14–19]. XRD provides non-destructive structural

characterisation typically of highly-ordered collagen fibrils; randomly oriented arrays lead to weak diffraction patterns and peak broadening [20–24]. Of these techniques, AFM can uniquely provide high-resolution imaging of collagen in physiological conditions and has been used to measure D periodicity and fibril size and organisation. Striking examples of imaging collagen fibrils without sample bleaching have been reported [25–27]; however, for certain samples, including extruded fibres, some chemical treatments (e.g., cross-linking [13] and bleaching [28, 29]) are needed to observe, e.g., D periodicity. While standard AFM modes can provide information on fibril alignment, they do not provide a measure of fibril polarity. Second harmonic generation (SHG) imaging is an optical technique that has been used in recent years to map polar organisation and determine fibril size without the need for surface treatments [30–32]; however, SHG is unable to resolve D periodicity. Similar to SHG, an AFM mode called lateral piezoresponse force microscopy (LPFM) can be used to map polar orientation and, in addition, reveal D periodicity and local electromechanical activity of collagen fibrils [33–36].

Electromechanical coupling in bone and collagenous tissues has been investigated extensively since the first report by Fukada and Yasuda [37]. Significant effort has been directed toward a complete understanding of how piezoelectricity in collagen-based materials, which was subsequently also found in many other biological systems, is related to bio-functionality [38–40]. LPFM is a contact mode, voltage-modulated AFM-based technique that detects bias-induced surface deformations via the converse piezoelectric effect [41]. LPFM allows evaluation of the piezoelectric properties of a wide variety of native and engineered biological materials [41, 42]. In this work, we utilise LPFM to determine fibril size, organisation, orientation, and D periodicity in extruded collagen fibres.

2. Material and methods

2.1. Collagen solution preparation

Type I collagen was extracted from bovine Achilles tendons following a protocol described previously [6]. Briefly, the tendons were suspended in 0.5 M acetic acid in the presence of pepsin (2,500 units/mg, Roche Diagnostics, UK) for 72 h at 4 °C. Acidic soluble collagen was filtered and purified by repeated salt precipitation (0.9 M NaCl) followed by centrifugation at 4°C for 45 min (Jouan Gr20.22, Thermo Electron Corporation, Bath, UK) and resuspended in 1 M acetic acid. The final collagen solution was obtained after dialysis (8,000 molecular weight cut off) against 0.01 M acetic acid and kept refrigerated until used. Collagen concentration was determined by hydroxyproline assay (3 mg/ml) and its purity (90% type I) was determined by sodium dodecyl sulphate–polyacrylamide gel electrophoresis analysis [43, 44].

2.2. Fibre extrusion procedure

Collagen fibre formation was based on previous work [45, 46] and produced as previously described [6, 10, 11]. Collagen solution was loaded into a 5 ml syringe and placed into a syringe pump system connected to a silicone tube of 1.5 mm internal diameter. Fibres were prepared by extruding the collagenous solution at a rate of 0.4 ml/min into a fibre formation buffer (118 mM phosphate buffer containing 20% poly(ethylene glycol); pH 7.50, 37 °C) for 10 min and were further incubated for 10 min in a fibre incubation buffer (6.0 mM phosphate buffer containing 75 mM sodium chloride; pH 7.10, 37 °C). Subsequently, the fibres were incubated overnight in phosphate buffered saline. Thereafter, the fibres were removed and thoroughly washed three times in distilled water and then were air-dried at room temperature. Some of the fibres were bleached with an aqueous solution of 4 vol% $NaOCl_{aq}$ for 20 s, thus exposing the fibrils at the fibre surface [28, 47].

2.3. SEM measurements

Field emission SEM (JEOL, JSM 7600F, at an accelerating voltage of 5 kV) was used to examine collagen fibres before and after bleaching. The fibre was fixed on the SEM sample holder and gold sputter-coated prior to imaging. The average width of 15 collagen fibril bundles or individual fibrils was determined from the full width at half maximum between minima of SEM image line profiles using ImageJ from both untreated and bleached samples.

2.4. AFM and PFM measurements

As collagen is a shear piezoelectric, LPFM was used to measure periodic in-plane sample deformation upon application of an AC voltage due to the converse piezoelectric effect. The resulting torsion of the cantilever and corresponding lateral movement of the laser on the photodetector was demodulated into amplitude and phase signals using a lock-in amplifier. The magnitude of the sample deformation can be inferred from the LPFM amplitude signal where larger surface deformations, related to higher piezoelectric coefficients, correspond to higher values. The phase signal represents in-phase or out-of-phase electromechanical response to the applied excitation voltage and allows the polar orientation of the sample to be determined [41].

The LPFM measurements were performed in ambient conditions, using an Asylum Research MFP-3D AFM equipped with a Zurich Instruments HF2LI lock-in amplifier. Prior to imaging, the collagen fibre was placed on a grounded copper substrate using conductive silver paint. An AC voltage (typically 30 V at 7 kHz) was applied using a high voltage amplifier power supply (F10A, FLC Electronics AB) via a conductive Pt-coated tip (Nanosensors, PPP-EFM) with a nominal resonant frequency and spring constant of 75 kHz and 2.8 N/m, respectively. LPFM phase images were corrected for phase wrapping when needed.

The average width of 30 collagen fibril domains was calculated from LPFM amplitude images as full width at half maximum between minima at boundaries between adjacent fibrils of opposite polarisation, in both untreated and bleached samples. The alignment of the collagen fibrils was quantitatively determined as the average anisotropy of LPFM amplitude images, from 3 different 5×5 μm^2 areas along both the bleached and unbleached fibres, on a scale between 0 (isotropic) and 1 (highly anisotropic) using the FibrilTool ImageJ plugin, which was developed to quantify the alignment fibrillar structures in an image [48].

3. Results and discussion

3.1. Collagen fibres before $NaOCl_{aq}$ treatment

SEM and AFM topography images of untreated collagen fibres (figure 1) displayed no clear distinction between individual fibrils; however, features parallel to the fibre (horizontal across the figure) in the SEM image likely represent bundles of fibres with an average width value of 222 ± 42 nm (Table 1). In the AFM topography image of a 5×5 μm^2 area (figure 2(a)) the alignment direction of the fibrils along the fibre was visible, but the average fibrillar width could not be determined. From the LPFM amplitude and phase images (figure 2(b) and (c), respectively), the collagen fibrillar structure was revealed to be organised into domains of uniform polarization with a significant degree of fibrillar alignment along the length of the fibre (anisotropy score [48] of 0.64 ± 0.03). Since the conductive probe is scanned in contact with a relatively soft surface, the increased tip-sample contact area can result in reduced image quality.

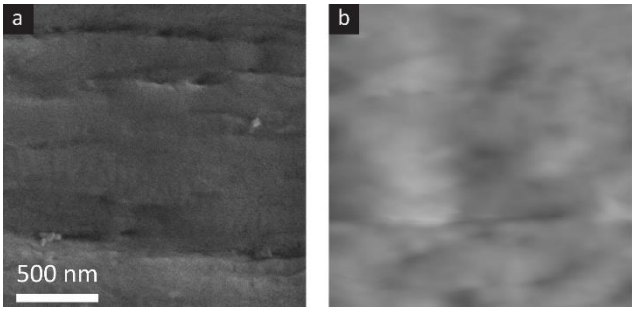

Figure 1. Collagen fibre before treatment. (a) SEM and (b) contact mode AFM topography images (z-scale = 180 nm) from different collagen fibres prior to bleaching.

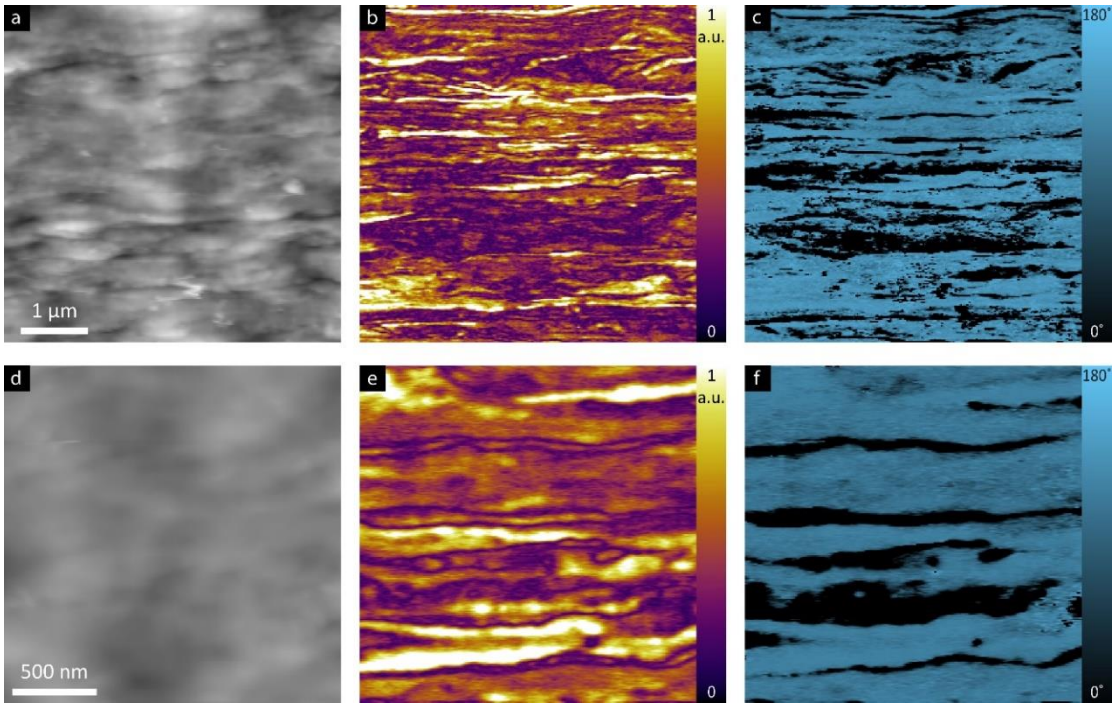

Figure 2. LPFM images of collagen fibre before treatment. (a) Contact mode AFM topography image (z-scale = 180 nm; scale bar = 1 µm) and corresponding (b) LPFM amplitude and (c) LPFM phase images of a collagen fibre. (d) Contact mode AFM topography image of smaller area taken from (a) (z-scale = 180 nm; scale bar = 0.5 µm). (e) LPFM amplitude and (f) LPFM phase image of area in (a).

The average fibrillar domain width was determined from the LPFM amplitude image in figure 2(b) to be 74 ± 18 nm (Table 1). The LPFM phase image, shown in figure 2(c), reveals the orientation of each domain, which is dependent on the direction of the polar bonds in collagen molecules from N to C termini. A change in phase of 180° indicates a change in domain orientation corresponding to the polar order of N and C groups, e.g., bright (dark) phase indicates N to C polarity is directed to the right (left). Domain boundaries, visible in the LPFM amplitude image in figure 2(e), coincide with the change in the polarization evident from the LPFM phase image in figure 2(f).

3.2. Collagen fibres after $NaOCl_{aq}$ treatment

After exposure to $NaOCl_{aq}$, collagen fibrils at the fibre surface were revealed. Exposure to $NaOCl_{aq}$ has been previously reported to enable visualisation of collagen fibrils in collagenous tissues [28]. In the bleached fibre, collagen fibrils with characteristic banding patterns were present (figures 3 and 4). The D periodicity was determined to be 66 ± 1 nm for both AFM and SEM images following the procedure outlined in Denning et al. [49]. The average fibril width of the bleached fibre was determined to be 70 ± 10 nm by SEM and 71 ± 19 nm by AFM (Table 1). In an extruded fibre, it is likely that fibrils will not reside neatly side by side, but be positioned slightly out of register in 3D. Therefore, they will have some degree of overlap, complicating the determination of fibril size, which would normally be determined by AFM height measurements of isolated fibrils in a liquid environment with low imaging forces to prevent dehydration and mechanical deformation. In this scenario, the measured width of the fibrils might be lower than the real fibril diameter. Note also that the tips used have a quoted tip radius of less than 25 nm; however, as the fibrils are tightly packed and the surface corrugation is not well-defined (figure 4(d) has a roughness of ~17 nm), the effects of tip broadening are minimised. Agreement between tipless SEM and AFM measurements further supports that tip convolution is negligible in these AFM measurements. The domain width measured from LPFM amplitude images after treatment (73 ± 19 nm) agrees with the LPFM measurement before bleaching and overlaps with the value obtained by AFM within statistical error. AFM and SEM measurements could underestimate the fibril diameter in extruded fibres in some samples and width measurements obtained by LPFM are likely more representative of the real fibril diameter since the minima in the LPFM amplitude images provide a clearer demarcation of the fibrils than is available in the topographic images.

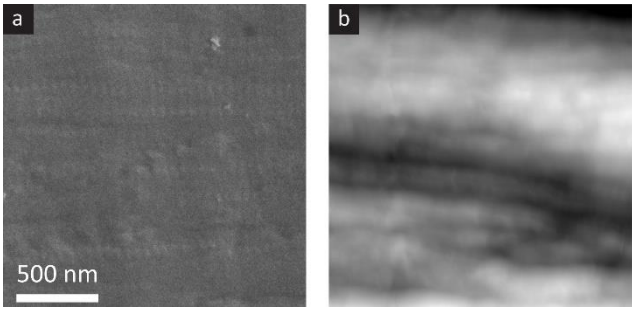

Figure 3. Collagen fibre after treatment. (a) SEM and (b) contact mode AFM topography images (z-scale = 180 nm) from different collagen fibres after bleaching.

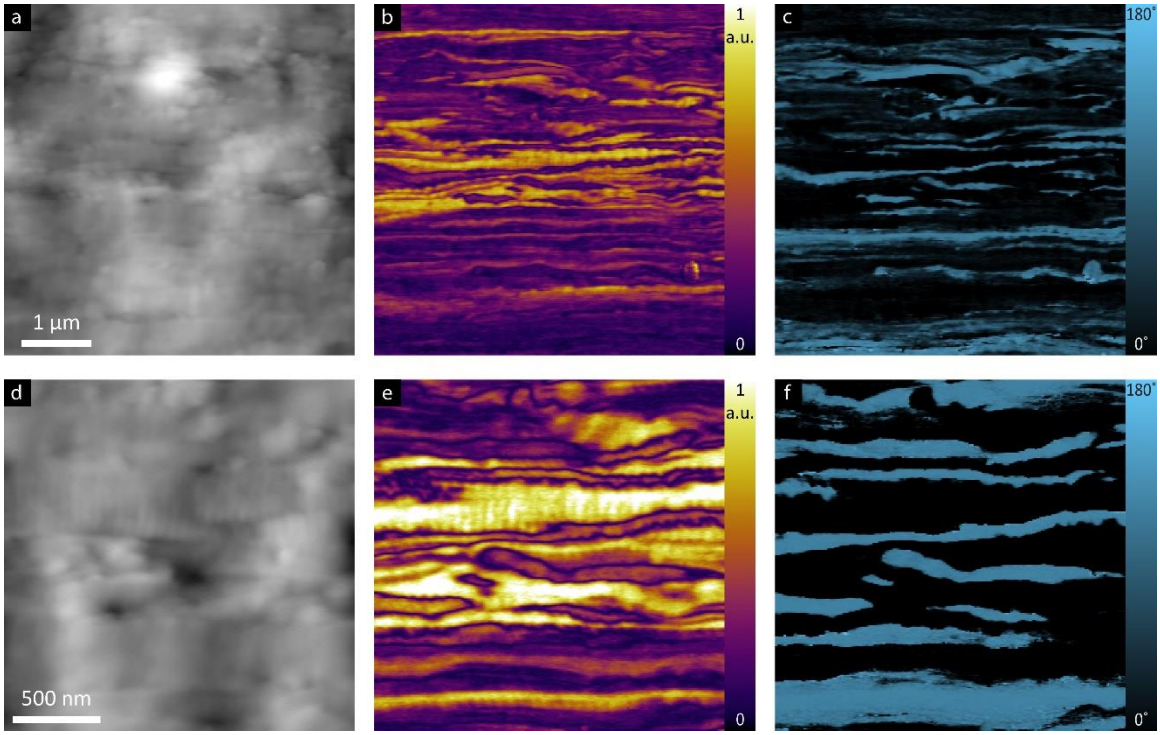

Figure 4. LPFM images of bleached (treated) collagen fibre. (a) AFM contact mode topography image (z-scale = 180 nm; scale bar = 1 µm). (b) LPFM amplitude and (c) LPFM phase image of area in (a). (d) AFM topography image of smaller area taken from (a) (z-scale = 180 nm; scale bar = 0.5 µm). (e) LPFM amplitude and (f) LPFM phase image of area in (a).

Polar ordering after bleaching is visible in the LPFM phase images (figure 4(c) and (f)). The fibrils show a high degree of alignment along the fibre with an anisotropy value 0.72 ± 0.01, indicating that bleaching did not drastically affect the fibril organisation or alignment. Thus, LPFM can reveal the fibril width without bleaching, providing a non-destructive measurement tool to determine fibril size, organisation, and orientation.

While this study has revealed the structure and organisation of collagen fibrils at the surface of the fibre using LPFM, the diameter of individual fibrils within the fibre could be reliably determined by measuring vertical piezoresponse of a fibre cross section, as has been previously shown for rat tail tendon [35]. The presented method can be extended to measure characteristic dimensions and organisation of any piezoelectric polymer or biopolymer, without the need for destructive chemical treatments.

Table 1. Determination of collagen fibril width from AFM, LPFM, and SEM images before and after bleaching.

Fibre	SEM [nm]	AFM topography [nm]	LPFM amplitude [nm]
Untreated	222 ± 42 *	–	74 ± 18
Bleached	70 ± 10	71 ± 19	73 ± 19

*corresponding to bundles of fibrils

4. Summary

The functional properties of engineered collagenous tissues are expected to depend on the size and organisation of the constituent collagen fibrils. Whereas collagen fibril size cannot be measured for some samples such as extruded collagen fibres, in standard AFM and SEM imaging without sample bleaching, the electromechanical properties of collagen provide a route to determine fibril size, organisation, and orientation without surface treatment. The fibril width obtained from LPFM amplitude images (74 ± 18 nm) of the untreated fibre agrees with the widths measured from the AFM topography (71 ± 19 nm), SEM (70 ± 10 nm), and LPFM amplitude (73 ± 19 nm) images of the bleached sample. Thus, LPFM can be used to measure collagen fibril widths in extruded collagen fibres without destructive chemical treatments.

Acknowledgements

This research was funded by the Ministry of Higher Education of Saudi Arabia under the King Abdullah Scholarship Program (IR10239). Part of this work was supported by Science Foundation Ireland (14/US/I3113, 13/RC/2073, and SFI07/IN1/B931), and the European Union's Horizon 2020 research and innovation program under Marie Skłodowska-Curie grant agreement number 644175. This work was further supported by the Teagasc Walsh Fellowship (2014045) and the ReValueProtein Research Project (11/F/043), supported by the Department of Agriculture, Food and the Marine (DAFM) under the National Development Plan 2007–2013, funded by the Irish Government. The authors acknowledge Dr. Ian Reid for assistance with SEM.

References

[1] Yee-Shuan Lee, L. Arinzeh T 2011 Electrospun Nanofibrous Materials for Neural Tissue Engineering. *Polymers (Basel)* **3** 413–426

[2] Koulikovska M, Rafat M, Petrovski G, Veréb Z, Akhtar S, Fagerholm P, Lagali N 2015 Enhanced Regeneration of Corneal Tissue via a Bioengineered Collagen Construct Implanted by a Nondisruptive Surgical Technique. *Tissue Eng Part A* **21** 1116–1130

[3] Lee SJ, Liu J, Oh SH, Soker S, Atala A, Yoo JJ 2008 Development of a composite vascular scaffolding system that withstands physiological vascular conditions. *Biomaterials* **29** 2891–2898

[4] Cen L, Liu W, Cui L, Zhang W, Cao Y 2008 Collagen tissue engineering: development of novel biomaterials and applications. *Pediatr Res* **63** 492–496

[5] Abu-Rub MT, Billiar KL, van Es MH, Knight A, Rodriguez BJ, Zeugolis DI, McMahon S, Windebank AJ, Pandit A 2011 Nano-textured self-assembled aligned collagen hydrogels promote directional neurite guidance and overcome inhibition by myelin associated glycoprotein. *Soft Matter* **7** 2770

[6] Zeugolis DI, Paul RG, Attenburrow G 2008 Factors influencing the properties of reconstituted collagen fibers prior to self-assembly: animal species and collagen extraction method. *J Biomed Mater Res A* **86** 892–904

[7] Zeugolis DI, Paul RG, Attenburrow G 2008 Post-self-assembly experimentation on extruded collagen fibres for tissue engineering applications. *Acta Biomater* **4** 1646–1656

[8] Enea D, Henson F, Kew S, Wardale J, Getgood A, Brooks R, Rushton N 2011 Extruded collagen fibres for tissue engineering applications: Effect of crosslinking method on mechanical and biological properties. *J Mater Sci*

Mater Med **22** 1569–1578

[9] Zeugolis DI, Paul RG, Attenburrow G 2009 Extruded Collagen Fibres for Tissue-Engineering Applications: Influence of Collagen Concentration and NaCl Amount. *J Biomater Sci Polym Ed* **20** 219–234

[10] Zeugolis DI, Paul GR, Attenburrow G 2009 Cross-linking of extruded collagen fibers-A biomimetic three-dimensional scaffold for tissue engineering applications. *J Biomed Mater Res Part A* **89A** 895–908

[11] Zeugolis DI, Paul RG, Attenburrow G 2010 The influence of a natural cross-linking agent (Myrica rubra) on the properties of extruded collagen fibres for tissue engineering applications. *Mater Sci Eng C* **30** 190–195

[12] Shepherd D V., Shepherd JH, Ghose S, Kew SJ, Cameron RE, Best SM 2015 The process of EDC-NHS cross-linking of reconstituted collagen fibres increases collagen fibrillar order and alignment. *APL Mater* **3** 14902

[13] Ahmad Z, Shepherd JH, Shepherd D V, Ghose S, Kew SJ, Cameron RE, Best SM, Brooks RA, Wardale J, Rushton N 2015 Effect of 1-ethyl-3-(3-dimethylaminopropyl) carbodiimide and N-hydroxysuccinimide concentrations on the mechanical and biological characteristics of cross-linked collagen fibres for tendon repair. *Regen Biomater* **2** 77–85

[14] Williams BR, Gelman RA, Poppke DC, Piez KA 1978 Collagen fibril formation. Optimal in vitro conditions and preliminary kinetic results. *J Biol Chem* **253** 6578–6585

[15] Hulmes DJ, Jesior JC, Miller A, Berthet-Colominas C, Wolff C 1981 Electron microscopy shows periodic structure in collagen fibril cross sections. *Proc Natl Acad Sci U S A* **78** 3567–3571

[16] Holmes DF, Lowe MP, Chapman JA 1994 Vertebrate (chick) collagen fibrils

formed in Vivo can exhibit a reversal in molecular polarity. *J Mol Biol* **235** 80–83

[17] Thurmond FA, Trotter JA 1994 Native collagen fibrils from echinoderms are molecularly bipolar. *J Mol Biol* **235** 73–79

[18] Kadler KE, Holmes DF, Trotter JA, Chapman JA 1996 Collagen fibril formation. *Biochem J* **316** 1–11

[19] Pins GD, Christiansen DL, Patel R, Silver FH 1997 Self-assembly of collagen fibers. Influence of fibrillar alignment and decorin on mechanical properties. *Biophys J* **73** 2164–2172

[20] Hulmes DJS, Miller A, White SW, Doyle BB 1977 Interpretation of the meridional X-ray diffraction pattern from collagen fibres in terms of the known amino acid sequence. *J Mol Biol* **110** 643–666

[21] Aspden RM, Hukins DWL 1979 Determination of the direction of preferred orientation and the orientation distribution function of collagen fibrils in connective tissues from high-angle X-ray diffraction patterns. *J Appl Crystallogr* **12** 306–311

[22] Wess TJ, Hammersley AP, Wess L, Miller A 1998 Molecular packing of type I collagen in tendon. *J Mol Biol* **275** 255–267

[23] Tsuruta H, Irving TC 2008 Experimental approaches for solution X-ray scattering and fiber diffraction. *Curr Opin Struct Biol* **18** 601–608

[24] Berenguer F, Bean RJ, Bozec L, Vila-Comamala J, Zhang F, Kewish CM, Bunk O, Rodenburg JM, Robinson IK 2014 Coherent X-ray imaging of collagen fibril distributions within intact tendons. *Biophys J* **106** 459–466

[25] Gutsmann T, Fantner GE, Venturoni M, Ekani-Nkodo A, Thompson JB, Kindt JH, Morse DE, Fygenson DK, Hansma PK 2003 Evidence that collagen fibrils

in tendons are inhomogeneously structured in a tubelike manner. *Biophys J* **84** 2593–2598

[26] Cisneros D a, Friedrichs J, Taubenberger A, Franz CM, Muller DJ 2007 Creating ultrathin nanoscopic collagen matrices for biological and biotechnological applications. *Small* **3** 956–963

[27] Wenger MPE, Bozec L, Horton MA, Mesquida P 2007 Mechanical properties of collagen fibrils. *Biophys J* **93** 1255–1263

[28] Habelitz S, Balooch M, Marshall SJ, Balooch G, Marshall GW 2002 In situ atomic force microscopy of partially demineralized human dentin collagen fibrils. *J Struct Biol* **138** 227–236

[29] Denning D, Abu-Rub MT, Zeugolis DI, Habelitz S, Pandit A, Fertala A, Rodriguez BJ 2012 Electromechanical properties of dried tendon and isoelectrically focused collagen hydrogels. *Acta Biomater* **8** 3073–3079

[30] Parry DAD, Craig AS 1977 Quantitative electron microscope observations of the collagen fibrils in rat-tail tendon. *Biopolymers* **16** 1015–1031

[31] Rivard M, Popov K, Couture C-A, et al 2014 Imaging the noncentrosymmetric structural organization of tendon with Interferometric Second Harmonic Generation microscopy. *J Biophotonics* **7** 638–646

[32] Couture C-A, Bancelin S, Van der Kolk J, et al 2015 The Impact of Collagen Fibril Polarity on Second Harmonic Generation Microscopy. *Biophys J* **109** 2501–2510

[33] Minary-Jolandan M, Yu M-F 2009 Nanoscale characterization of isolated individual type I collagen fibrils: polarization and piezoelectricity. *Nanotechnology* **20** 85706

[34] Harnagea C, Vallières M, Pfeffer CP, Wu D, Olsen BR, Pignolet A, Légaré F,

Gruverman A 2010 Two-Dimensional Nanoscale Structural and Functional Imaging in Individual Collagen Type I Fibrils. *Biophys J* **98** 3070–3077

[35] Denning D, Alilat S, Habelitz S, Fertala A, Rodriguez BJ 2012 Visualizing molecular polar order in tissues via electromechanical coupling. *J Struct Biol* **180** 409–419

[36] Denning D, Paukshto M V., Habelitz S, Rodriguez BJ 2014 Piezoelectric properties of aligned collagen membranes. *J Biomed Mater Res - Part B Appl Biomater* **102** 284–292

[37] Fukada E, Yasuda I 1957 On the Piezoelectric Effect of Bone. *J Phys Soc Japan* **12** 1158–1162

[38] Bassett CA, Pawluk RJ 1972 Electrical behavior of cartilage during loading. *Science* **178** 982–983

[39] Athenstaedt H 1974 Pyroelectric and piezoelectric properties of vertebrates. *Ann N Y Acad Sci* **238** 68–94

[40] Lang SB 2000 Piezoelectricity, pyroelectricity and ferroelectricity in biomaterials: Speculation on their biological significance. *IEEE Trans Dielectr Electr Insul* **7** 466–473

[41] Denning D, Guyonnet J, Rodriguez BJ 2016 Applications of piezoresponse force microscopy in materials research: from inorganic ferroelectrics to biopiezoelectrics and beyond. *Int Mater Rev* **61** 46–70

[42] Rodriguez BJ, Kalinin SV, Shin J, Jesse S, Grichko V, Thundat T, Baddorf AP, Gruverman A 2006 Electromechanical imaging of biomaterials by scanning probe microscopy. *J Struct Biol* **153** 151–159

[43] Reddy GK, Enwemeka CS 1996 A simplified method for the analysis of hydroxyproline in biological tissues. *Clin Biochem* **29** 225–229

[44] Laemmli UK 1970 Cleavage of structural proteins during the assembly of the head of bacteriophage T4. *Nature* **227** 680–685

[45] Cavallaro JF, Kemp PD, Kraus KH 1994 Collagen fabrics as biomaterials. *Biotechnol Bioeng* **44** 146

[46] Wang MC, Pins GD, Silver FH 1994 Collagen fibres with improved strength for the repair of soft tissue injuries. *Biomaterials* **15** 507–512

[47] Marshall GW, Yücel N, Balooch M, Kinney JH, Habelitz S, Marshall SJ 2001 Sodium hypochlorite alterations of dentin and dentin collagen. *Surf Sci* **491** 444–455

[48] Boudaoud A, Burian A, Borowska-Wykręt D, Uyttewaal M, Wrzalik R, Kwiatkowska D, Hamant O 2014 FibrilTool, an ImageJ plug-in to quantify fibrillar structures in raw microscopy images. *Nat Protoc* **9** 457–463

[49] Denning D, Kilpatrick JI, Hsu T, Habelitz S, Fertala A, Rodriguez BJ 2014 Piezoelectricity in collagen type II fibrils measured by scanning probe microscopy. *J Appl Phys* **116** 66818

Figure captions

Figure 5. Collagen fibre before treatment. (a) SEM and (b) contact mode AFM topography images (z-scale = 180 nm) from different collagen fibres prior to bleaching.

Figure 6. LPFM images of collagen fibre before treatment. (a) Contact mode AFM topography image (z-scale = 180 nm; scale bar = 1 μm) and corresponding (b) LPFM amplitude and (c) LPFM phase images of a collagen fibre. (d) Contact mode AFM topography image of smaller area taken from (a) (z-scale = 180 nm; scale bar = 0.5 μm). (e) LPFM amplitude and (f) LPFM phase image of area in (a).

Figure 3. Collagen fibre after treatment. (a) SEM and (b) contact mode AFM topography images (z-scale = 180 nm) from different collagen fibres after bleaching.

Figure 4. LPFM images of bleached (treated) collagen fibre. (a) AFM contact mode topography image (z-scale = 180 nm; scale bar = 1 μm). (b) LPFM amplitude and (c) LPFM phase image of area in (a). (d) AFM topography image of smaller area taken from (a) (z-scale = 180 nm; scale bar = 0.5 μm). (e) LPFM amplitude and (f) LPFM phase image of area in (a).

Figures

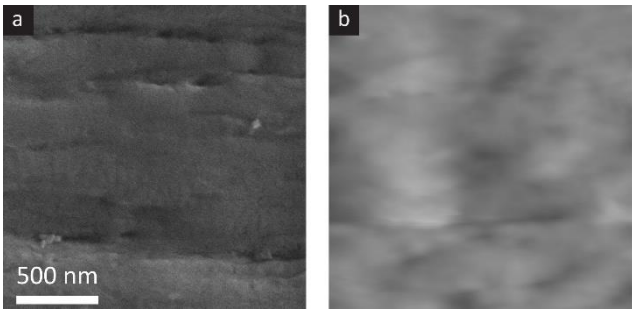

Figure 1, Bazaid et al.

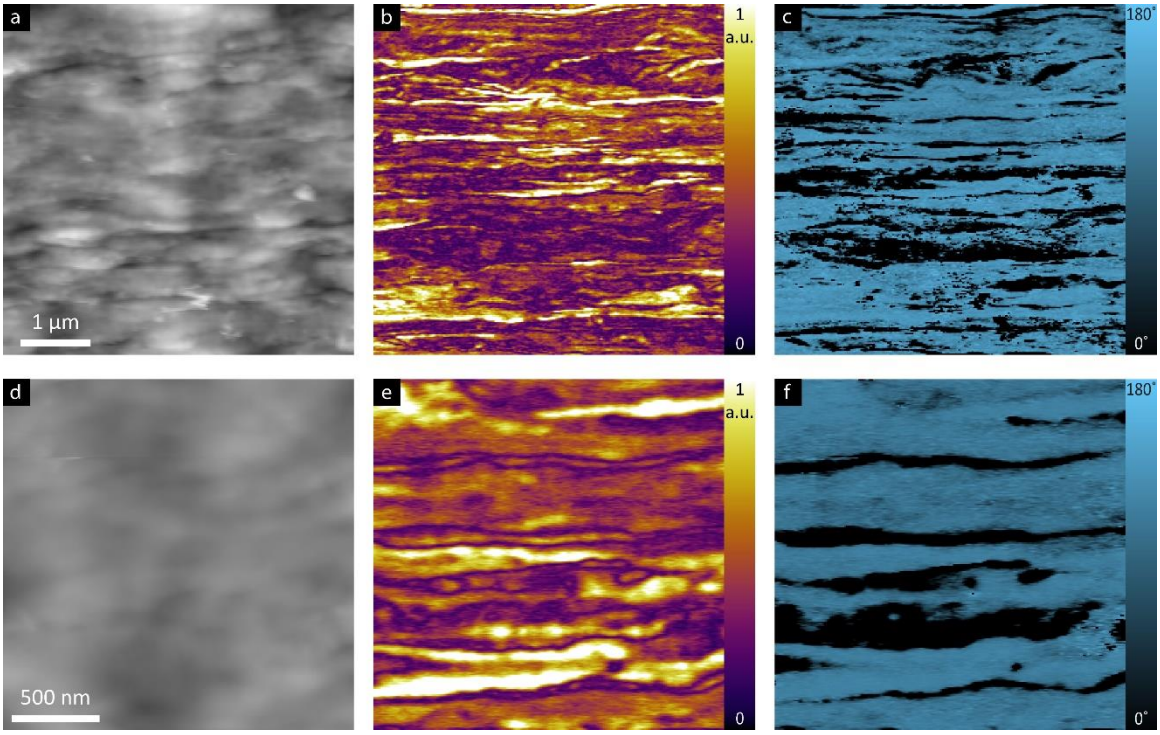

Figure 2, Bazaid et al.

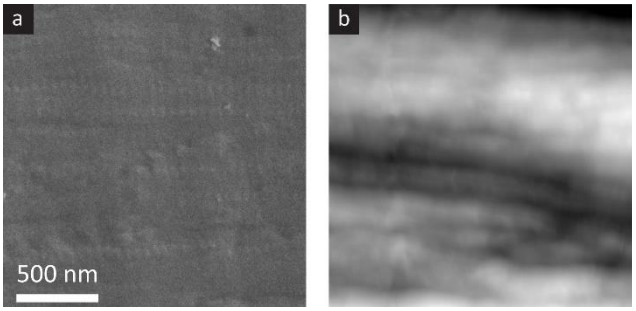

Figure 3, Bazaid et al.

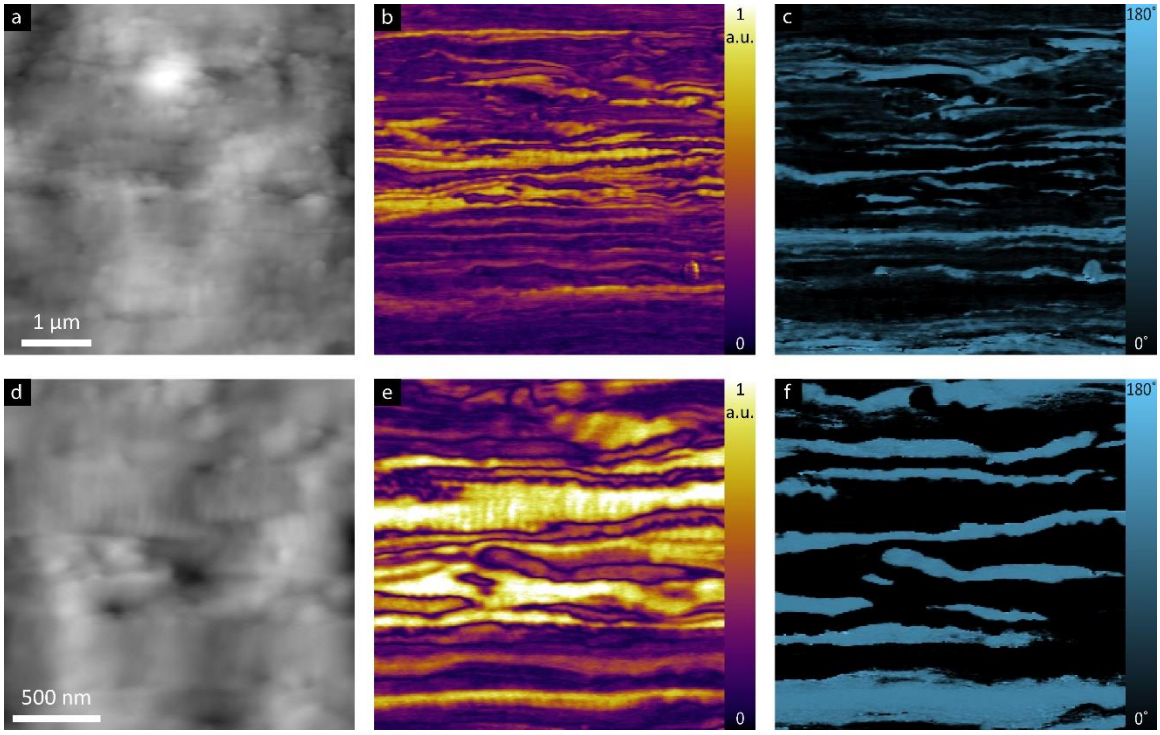

Figure 4, Bazaid et al.